

GTINDIA2012-9645

**THERMODYNAMIC OPTIMIZATION AND OFF-DESIGN PERFORMANCE ANALYSIS
OF A TOLUENE BASED RANKINE CYCLE FOR WASTE HEAT RECOVERY
FROM MEDIUM-SIZED GAS TURBINES**

Carlo Carcasci, Riccardo Ferraro

“S. Stecco” Department of Energy Engineering
University of Florence
Via Santa Marta, 3
50139 Florence ITALY
carlo.carcasci@unifi.it; riccardo.ferraro@unifi.it

ABSTRACT

In the last years, the accelerated consumption of fossil fuels has caused many serious environmental problems such as global warming, the depletion of the ozone layer and atmospheric pollution. Similarly, low-temperature waste heat which is discharged in several industrial processes, contributes to thermal pollution and damages the environment. Furthermore, many industrial applications use low enthalpy thermal sources, where the conventional systems for the conversion of thermal energy into electrical energy, based on a Rankine water cycle, work with difficulty. Thus, the Organic Rankine Cycle can be considered a promising process for the conversion of heat at low and medium temperature whenever the conventional water cycle causes problems. Using an organic working fluid instead of water, the ORC system works like the bottom cycle of a conventional steam power plant. This kind of cycle allows a high utilization of the available thermal source. Moreover, the choice of the working fluid is critical, because it should meet several environment standards and not only certain thermophysical properties.

This paper illustrates the results for the simulations of an Organic Rankine Cycle based on a gas turbine with a diathermic oil circuit. The selected working fluid is toluene. The design is performed with a sensitivity analysis of the main process parameters, the organic Rankine cycle is optimized by varying the main pressure of the fluid at different temperatures of the oil circuit. The off-design is performed by varying the temperature of the air condenser.

NOMENCLATURE

| | | |
|--------------|--|----------------------|
| a | Exponent of Heat transfer correlation | |
| f | fraction of thermal resistance | [-] |
| $(k/s)^{-1}$ | conduction thermal resistance in the metal | [m ² K/W] |
| m | mass flow rate | [kg/s] |
| Nu | Nusselt number | |
| P | Pressure | [bar] |
| R | Thermal resistance | [m ² K/W] |
| Re | Reynolds number | |
| T | Temperature | [°C – K] |
| U | Heat transfer coefficient | [W/m ² K] |
| W | Power | [kW] |

Greek

η Efficiency

Acronyms

| | |
|-----|------------------------------------|
| CON | Condenser |
| ECO | Economizer |
| EV | Evaporator |
| EX | Expander |
| GT | Gas Turbine |
| HRB | Hot Gas-Oil - Heat Recovery Boiler |
| ORC | Organic Rankine Cycle |
| REC | Recuperator/Regenerator |
| SH | Superheater |

Subscript

| | |
|------|--------------------------|
| air | Air in ambient condition |
| amb | Ambient |
| app | Approach |
| con | Condenser |
| cond | Conduction |
| des | Design |
| el | Electric |
| ex | Expander |
| exh | Exhaust from Gas Turbine |
| ext | External |
| fan | Fan |
| fl | Organic Fluid (Toluene) |
| in | inlet |
| int | Internal |
| lim | limit |
| max | Maximum |
| ml | Log mean difference |
| off | Off Design |
| oil | Oil |
| opt | optimized |
| pp | Pinch point |
| rid | non-dimensional |
| sat | saturation |
| st | Stack |
| sub | Subcooling |

INTRODUCTION

In the past decades, the increasing consumption of fossil fuels has caused many environmental problems such as global warming, the depletion of the ozone layer and atmospheric pollution. In addition, the discharged waste heat contributes to thermal pollution and therefore it too becomes an environmental problem. [1]. A study shows that more than 50% of the total heat generated in industry is low/medium grade heat which has been discharged as thermal pollution [2]. Moreover, the growing delocalization of the generation systems leads to the installation of small/medium-sized power plants with high efficiency. Under these conditions the use of aeroderivative gas turbines allows higher efficiency, but low/medium temperature waste heat. Due to all these reasons, utilizing low-grade waste heat for energy production has attracted more attention due to its potential rather than the actual reduction in fossil fuel consumption. When utilizing low/medium temperature waste heat, the performance of the traditional steam Rankine cycle is not satisfying due to its low thermal efficiency and large volume flows. Thus, others power plant configurations are studied, i.e. Carcasci et al. [3,4] have studied CRGT cycle. As one of the promising technologies for converting low/medium grade heat into electricity, the organic Rankine cycle (ORC) power plant has proved to be an attractive solution. Some research and development have been made in recent years, particularly on two important topics: thermodynamic analysis and working fluid selection. Waste heat recovery ORCs have been studied in

a number of previous works: Badr et al. [5], Gu et al. [6], Dai et al. [7], used simple thermodynamic models with constant pump and expander efficiencies to compare different candidate working fluids. In these studies the reliance of the efficiency on the evaporating pressure is shown. Particularly, there are studies that describe the parametric optimization and performance analysis of waste heat recovery from low grade sources [8, 9]. Advanced cycle configurations have been studied: Gnutek et al. [10] proposed an ORC cycle with multiple pressure levels and sliding vane expansion machines in order to maximize the use of the heat source; Chen et al. [11] studied the transcritical CO₂ power cycle. Several ORC bottoming cycles are analyzed in relation with solar applications [12-14], geothermal heat sources [15, 16], high temperature fuel cells [17] and heat recovery from gas turbines. Chacartegui et al. [18, 19] showed a parametric optimization of a combined cycle with a gas turbine and an ORC low temperature bottoming cycle, in order to achieve a better integration between these two technologies and then did a part-load analysis of a combined cycle based on a gas turbine and an ORC.

The organic fluids are categorized into three groups based on their slope of saturation vapor curves in the T-S diagram: fluids with a positive slope are dry fluids, fluids with a negative slope are wet fluids and fluids with nearly infinitely large slopes of saturated vapor curves are isentropic fluids. In their studies Lai et al. [20] and Sahleh et al. [21] conducted a thorough review of working fluids for low and high temperature organic Rankine cycles. Chacartegui et al. [18] presented toluene as one of the most interesting fluids. Vankeirsbilck et al. [22] showed a high efficiency regenerative cycle based on toluene. Other works presented some applications based on the use of toluene [23, 24]. Particular attention has been paid to the expander. Experimental studies of small scale ORC units demonstrated that the scroll expander is a good candidate for small scale power generation because of its reduced number of moving parts, its reliability, wide output power range, and broad availability [25, 26]. The isentropic effectiveness ranges from 48% to 65%, depending on the design of the scroll expander [27-30]. Del Turco et al. [31] presented an organic Rankine cycle with a double supersonic stage turboexpander covering a large power range. A recovery cycle based on cyclopentane with diathermic oil is shown. The first loop is used to carry the heat released from the gas turbine into the heat exchanger system, where energy is transferred to the working fluid. The second loop is the main thermodynamic cycle, where the organic fluid vaporizes. A superheater before the expander and a recuperator downstream the expander are positioned in the cycle.

In the present paper an organic Rankine cycle based on toluene is simulated. A thermodynamic cycle with a regenerator and a superheater is selected. In particular, the use of the superheater is evaluated and compared using several approach temperature differences ($\Delta T_{app}=T_B-T_1$).

Some fluids with specific characteristics, such as highly inflammable fluids, need diathermic oil to transfer heat from the exhaust gas to the working fluid. Common commercial

| | |
|---------------|-----------|
| W_{GTel} | 11250 kW |
| η_{GTel} | 31.4% |
| m_{GTel} | 47.5 kg/s |
| T_{GTel} | 482.°C |

TABLE 1:GE10-1 main specification [31]

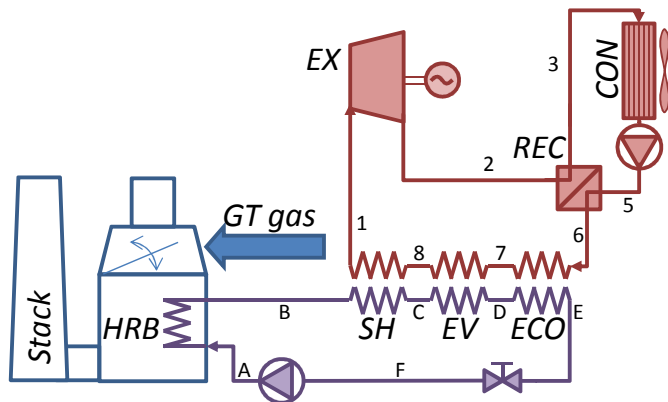


FIGURE 1: ORC POWER PLANT LAYOUT.

diathermic oils can reach up to 400°C [32]. The cycle is simulated by three different diathermic oil temperatures $T_B=360^\circ\text{C}$, 380°C and 400°C to evaluate the influence of the heat transfer recovery on the cycle output.

At last, the optimization of the cycle is presented by varying the expander inlet pressure and an off-design analysis by varying the ambient temperature in the condenser (CON). The gas turbine considered is the GE10-1 from General Electric – Nuovo Pignone, which is a heavy duty single shaft used for oil and gas or power generation applications [33]. Table 1 shows the main GE10-1 specification.

WORKING FLUID

The working fluid is toluene, $\text{C}_6\text{H}_5\text{CH}_3$ ($M_w=92.1$ kg/kmol), a water-insoluble liquid. It is an aromatic hydrocarbon that is widely used as an industrial feedstock and as a solvent. The high value of the critical temperature (591.8 K) and critical pressure (41.1 bar) allows to define toluene as one of the most interesting fluids in the ORC application recovery of waste heat from a gas turbine.

Although it is classified as a hazard fluid, it is much less toxic than benzene. Its inflammable temperature limit is relatively high (535°C), with a TLV (Threshold Limit Value) of 50 mL m^{-3} and 190 mg m^{-3} .

To simulate, the behavior of toluene, NIST software is used. The thermodynamic properties of toluene are obtained to reach critical value points of pressure and temperature.

Toluene is a dry fluid with a positive slope of the saturated vapor curve. According to the NIST library, the pressure where the vapor saturation entropy is maximum can be determined (about 36.bar). If the working pressure is above this value, the expansion line can present wet vapor.

| | | |
|-----------------------|------------|---|
| $T_{oil_max}=T_B$ | = 380.0 °C | (360°C-400°C for design) |
| $P_{ex_in}=P_1$ | = 36.0 bar | optimization in design |
| η_{HRB} | = 0.98 | |
| ΔT_{pp_HRB} | = 10.0 °C | |
| ΔT_{app} | = 30.0 °C | |
| ΔT_{pp} | = 8.0 °C | |
| η_{ex} | = 0.85 | |
| $\eta_{gearbox}$ | = 0.98 | |
| η_{el} | = 0.96 | |
| T_{air_in} | = 15.0 °C | |
| ΔT_{air_con} | = 20.0 °C | ($\rightarrow T_{air_out}=35.0^\circ\text{C}$) |
| ΔT_{pp_con} | = 20.0 °C | |
| ΔT_{pp_rec} | = 15.0 °C | |
| ΔT_{sub} | = 15.0 °C | |
| η_{pump} | = 0.70 | |

TABLE 2:ORC DATA SHEET

POWER PLANT SCHEME

The ORC cycle is based on the traditional subcritical Rankine cycle, which is applied to a bottoming cycle. Figure 1 shows the power plant scheme.

For safety reasons, the recovery cycle is designed by exploiting intermediary diathermic oil. This oil transfers heat of the hot exhaust gas from the gas turbine GT to the organic fluid (toluene). Firstly, the plant configuration of the reviewed cycle has only one level of evaporating pressure with the internal heat exchanger (recuperator REC) and a superheater (SH) to carry the fluid in the superheated vapor region. The hot exhaust gas goes into the first heat recovery unit (HRB), where the diathermic oil is heated. In the second loop the hot oil goes into the second heat recovery unit, composed by a superheater (SH), evaporator (EV) and an economizer (ECO) where a heavy hydrocarbon fluid is heated. The organic fluid (toluene) vaporizes in the exchanger unit and expands in an expander (EX). The exhaust fluid leaves the expander and enters into a recuperator (REC) that increases the system's efficiency [20]. At last, the fluid is cooled in a condenser (CON) and then pressurized in a pump. The condenser (CON) is air-cooled, and is mainly used for waterless areas.

THERMODYNAMIC AND DESIGN APPROACH

In the HRB recovery unit, the flow rate and the temperature of the exhaust hot gas (m_{GTel} , T_{GTel} . See table 1) from gas turbine are imposed. The maximum oil temperature (oil characteristic limit; $T_B=T_{oilMax}$) and the pinch point are imposed. The stack hot gas temperature (T_{st}) and the oil mass flow rate (m_{oil}) can be determined with the energy balance inside the HRB.

The inlet expander pressure (P_1), the approach temperature difference ($\Delta T_{app}=T_B-T_1$) and the pinch point temperature

difference ($\Delta T_{pp} = T_D - (T_7 + \Delta T_{sub})$) are imposed to determine the toluene mass flow ($m_{\dot{t}}$) and maximum temperature ($T_{ex_in} = T_1$) exploiting the energy balance inside the SH+EV.

The discharge pressure at the expander exit (P_2) can be determined considering the air condenser (CON): the ambient air temperature is known; by imposing a pinch point temperature difference in the condenser ($\Delta T_{pp_con} = T_{sat} - T_{air_out}$) it is possible to evaluate the saturated temperature of the toluene (T_{sat}) and so its pressure is determined (P_3). The air mass flow rate (m_{air}) necessary to cool the toluene is determined by imposing the inlet/outlet temperature difference ($\Delta T_{air_con} = T_{air_out} - T_{air_in}$) of the condenser air. Thus, the power absorbed by the fan (W_{fan}) can also be determined.

Both the inlet conditions at the expander and the discharge pressure are determined. Imposing the expander efficiency (η_{ex}), the output power (W_{ex}) and the toluene exhaust conditions can be determined.

In the recuperator (REC), the energy balance equations can be used. The pinch point temperature difference (ΔT_{pp_con}) is imposed to evaluate the inlet conditions of the condenser and the conditions of the toluene in the HRSG.

By exploiting the energy balance in the economizer of the HRSG (with an imposed ΔT_{sub} to forestall boiling in the economizer) the oil exhaust temperature (T_E) is determined. This data is necessary to achieve an energy balance in the oil HRB (see above). At the end of the thermodynamic evaluation, some parameters such as the log-mean temperature difference (ΔT_{ml}) and UA for each exchanger, the non-dimensional mass flow and pressure ratio for the expander can be determined.

OFFDESIGN ANALYSIS

As off-design working condition is considered the variation of the ambient temperature and its effect on the bottoming cycle.

When the plant works in off-design conditions, the temperature difference between the hot and the cold fluid cannot be exploited, but the surface (UA) must be imposed. In addition, the inlet hot gas, the oil pressure and the maximum oil temperature are selected.

The non-dimensional mass flow in the expander and the exhaust pressure (by condenser balance) can be determined, but they depend on the characteristics of the expander. This can be done in two ways: working with a fixed expander non-dimensional flow, so the inlet pressure varies (the inlet pressure is set by the expander's characteristic, in fact, the expander is often choked, so the non-dimensional flow ($m_{rid} = m_{ex} \cdot (T_{ex_in})^{0.5} / P_{ex_in} = \text{const}$) is constant, compared to the design conditions [19]). Otherwise the expander must be equipped with a control system (inlet valve) that sets the expander at the maximum imposed pressure. The isentropic efficiency depends on the expander operation conditions, and so the toluene exhaust conditions can be determined.

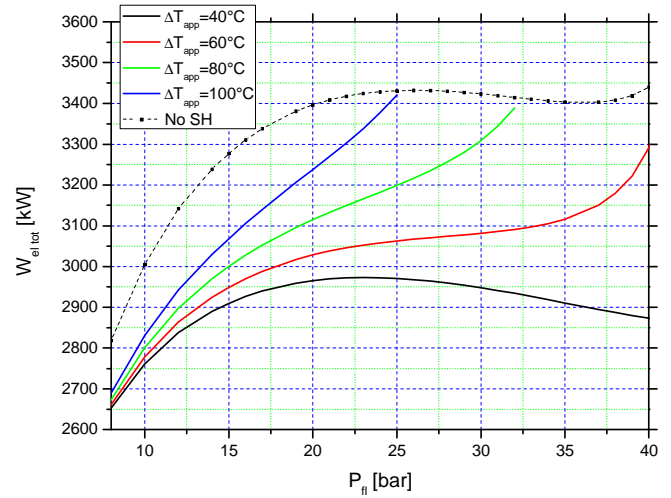


FIGURE 2: ELECTRIC OUTPUT POWER VERSUS EXPANDER INLET PRESSURE AND APPROACH TEMPERATURE DIFFERENCE.

Applying the energy balance and the heat transfer equations to the recuperator (REC), the inlet toluene conditions in the condenser (CON) and the economizer (ECO) can be determined.

The ambient conditions are known, by exploiting the energy balance, the surface of the condenser (UA) and the air mass flow rate, which determine the outlet air temperature (T_{air_out}) can be determined. The air mass flow rate of the fan condenser (m_{air}) is calculated by the energy balance in the condenser.

At this point, the economizer and evaporator inlet conditions can be determined.

Thus, the oil and the toluene loop are closed. The design and off-design conditions need a mass balance to check the equality of the design mass value, otherwise the plant needs a tank to compensate the fluctuations in the system. In the present study, mass conservation is not considered.

Heat Transfer Coefficient in Off-Design Condition

Three different parts make up the global heat transfer coefficient: internal, external and conduction in the metal.

$$U^{-1} = \frac{1}{U_{int}} + \frac{1}{k/s} + \frac{1}{U_{ext}} \quad [1]$$

Thermal resistance is considered. Each thermal factor is a fraction of the global thermal resistance.

$$f_{int} = \frac{R_{int}}{R} = \frac{U}{U_{int}} \quad f_{ext} = \frac{R_{ext}}{R} = \frac{U}{U_{ext}} \quad f_{cond} = \frac{R_{cond}}{R} = \frac{U}{k/s}$$

where

$$f_{int} + f_{cond} + f_{ext} = 1. \quad [3]$$

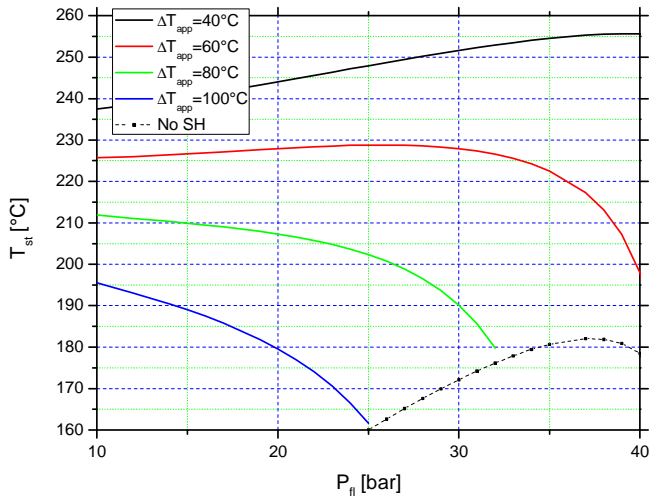


FIGURA 3: STACK TEMPERATURE VERSUS EXPANDER INLET PRESSURE AND APPROACH TEMPERATURE DIFFERENCE.

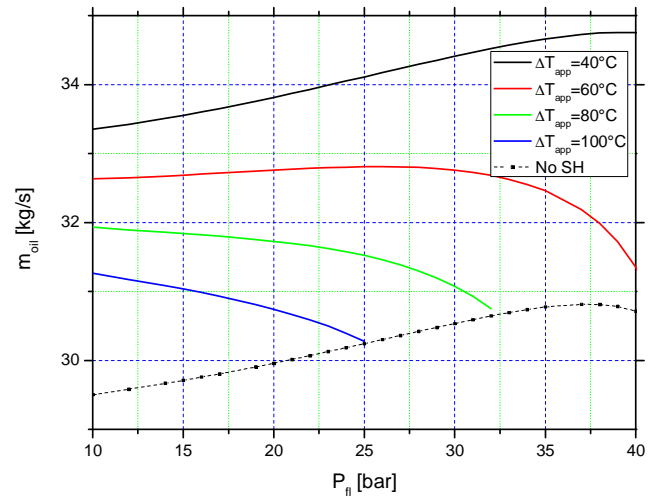


FIGURE 5: OIL MASS FLOW RATE VERSUS EXPANDER INLET PRESSURE AND APPROACH TEMPERATURE DIFFERENCE.

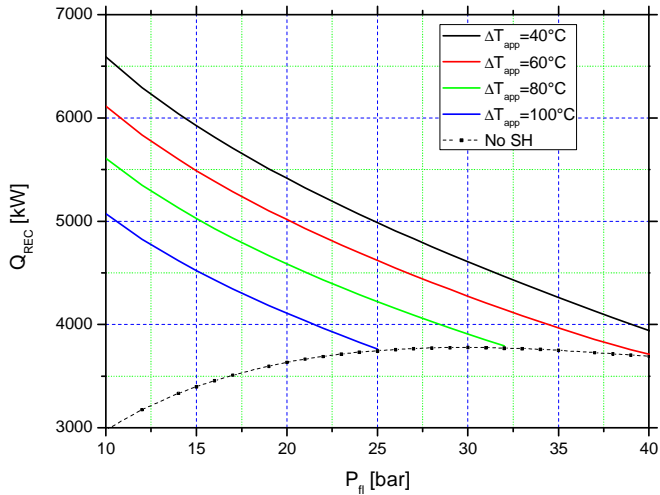


FIGURE 4: RECOVERED HEAT VERSUS EXPANDER INLET PRESSURE AND APPROACH TEMPERATURE DIFFERENCE.

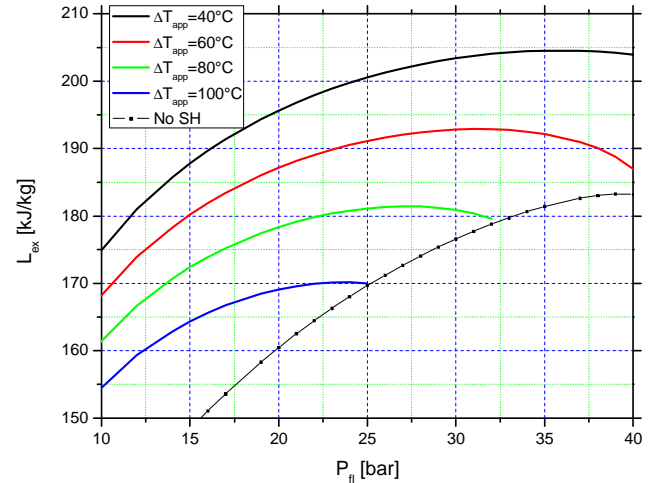


FIGURE 6: ENTHALPY DROP VERSUS EXPANDER INLET PRESSURE AND APPROACH TEMPERATURE DIFFERENCE.

Each factor can be selected exploiting previous experiences and the global heat transfer coefficient can be determined.

In an off-design analysis the HTC depends on the mass flow rate and on the fluid properties. Usually, a correlation for the heat transfer coefficient can be defined using Nusselt and Reynolds number [32] (where the exponent “a” is between 0.5-0.8).

$$Nu = C \cdot Re^a \rightarrow U \propto m^a \rightarrow \frac{U_{off}}{U_{des}} \propto \left(\frac{m_{off}}{m_{des}} \right)^a \quad [4]$$

Thus, with the mass flow rate, the heat transfer coefficient of each contribution can be determined. At this point, the global

heat transfer coefficient can be calculated using the equation (1).

THERMODYNAMIC AND DESIGN RESULTS

In this paper, the main thermodynamics parameters are analyzed. Table 2 illustrates the used values for the sensibility analysis.

Supereheater Considerations

Some papers [31, 35 and 36] present an ORC with the superheater, while other studies analyze a not-superheated cycle [18, 19]. This paper conducts a sensibility analysis, fixing the maximum oil temperature ($T_{oil_max}=T_B=380^\circ\text{C}$) and varying the

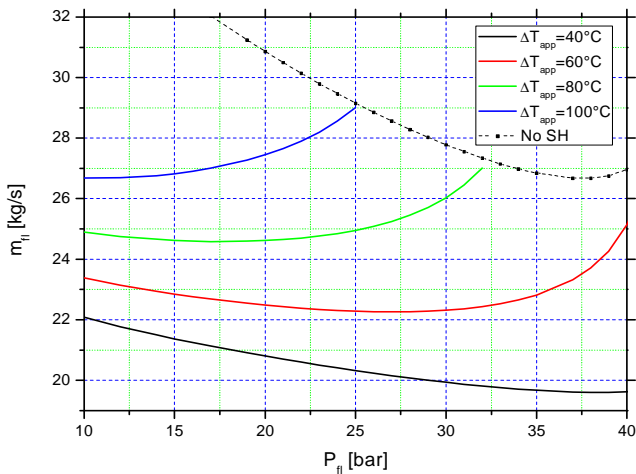


FIGURE 7: TOLUENE MASS FLOW RATE VERSUS EXPANDER INLET PRESSURE AND APPROACH TEMPERATURE DIFFERENCE.

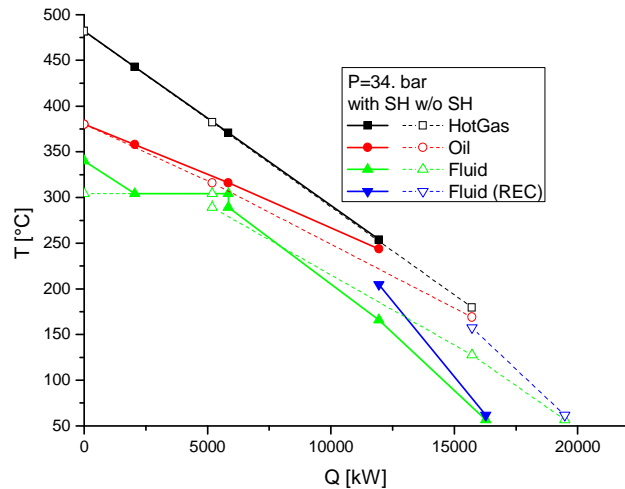


FIGURE 8: COMPARISON BETWEEN SUPERHEATED AND NO-SUPERHEATED LAYOUT.

approach temperature difference in the superheater (ΔT_{app}) and fluid pressure is conducted (figure 2). Fixing the ΔT_{app} , the output power increases with the fluid temperature. When the approach temperature difference (ΔT_{app}) is low, a maximum value is presented. Increasing the temperature difference, the output power (W_{el}) increases until the temperature difference is so high to correspond to a not-superheated condition. Increasing the fluid temperature and the ΔT_{app} , the heat recovery by the exhaust gas increases, in fact, the stack temperature decreases (figure 3).

Figure 4 shows the heat recovery in the recuperator (REC): it increases using low fluid pressure and high fluid temperature (low approach temperature difference). When the fluid pressure is further decreased or the maximum fluid temperature increased, the economizer becomes unnecessary; in fact, the fluid output conditions in the economizer are fixed by the fluid

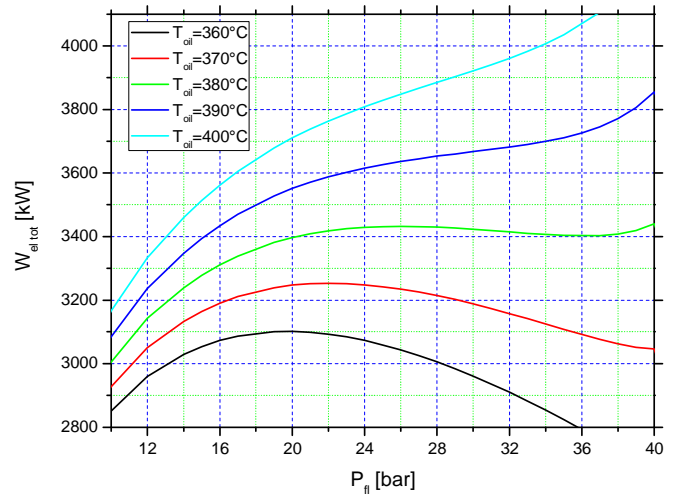


FIGURE 9: ELECTRIC OUTPUT POWER VERSUS EXPANDER INLET PRESSURE AND OIL TEMPERATURE.

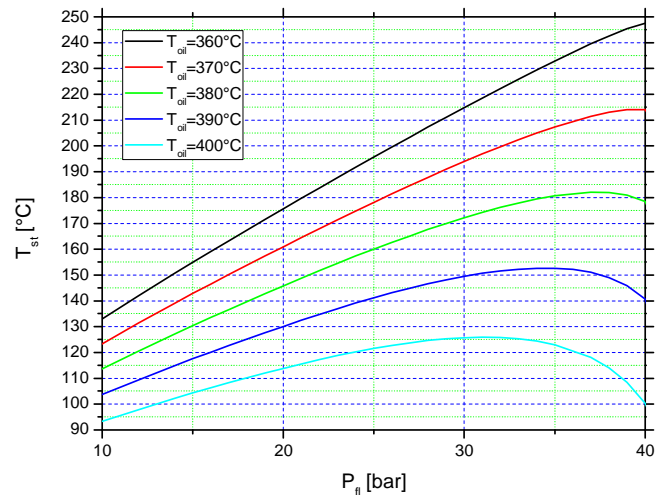


FIGURE 10: STACK TEMPERATURE VERSUS EXPANDER INLET PRESSURE AND OIL TEMPERATURE.

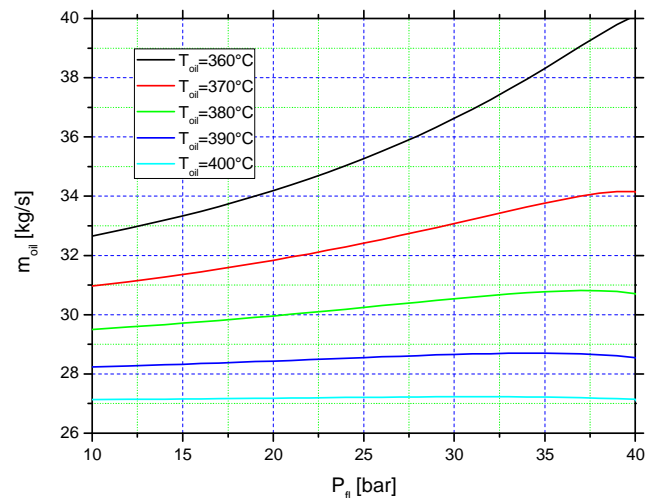


FIGURE 11: OIL MASS FLOW RATE VERSUS EXPANDER INLET PRESSURE AND OIL TEMPERATURE.

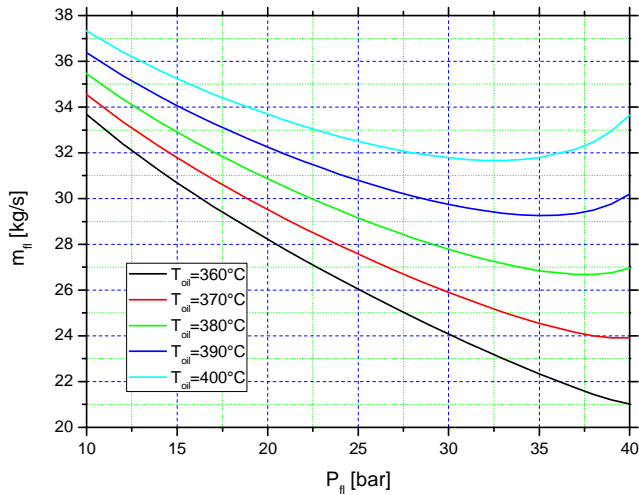


FIGURE 12: TOLUENE MASS FLOW RATE VERSUS EXPANDER INLET PRESSURE AND OIL TEMPERATURE.

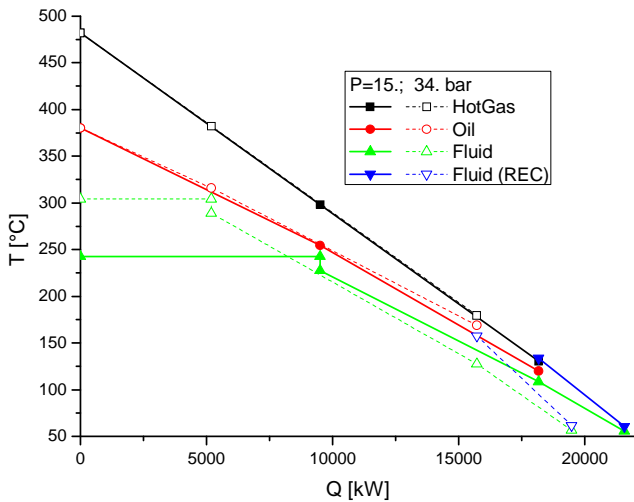


FIGURE 13: TS DIAGRAM - COMPARISON BETWEEN DIFFERENT PRESSURE VALUE.

pressure and the subcooling difference and boiling phenomena may happen in the recuperator. The oil that reaches the HRB, is hot and the exhaust gas temperature is high. Figure 5 shows the oil mass flow rate, which increases with the fluid maximum temperature and is quite constant with the inlet fluid pressure.

Increasing the working fluid pressure, the expander inlet enthalpy increases and the specific work at the condenser tends to increase (figure 6). Decreasing the approach temperature difference, the working fluid temperature and the specific work at the expander increase. This trend is not uniform because the discharge conditions from the expander are superheated. Without the superheater, the specific work at the expander is less, but the fluid mass flow rates tend to increase (figure 7). The trend of the figures 6 and 7 explain the non-linearity in figure 2.

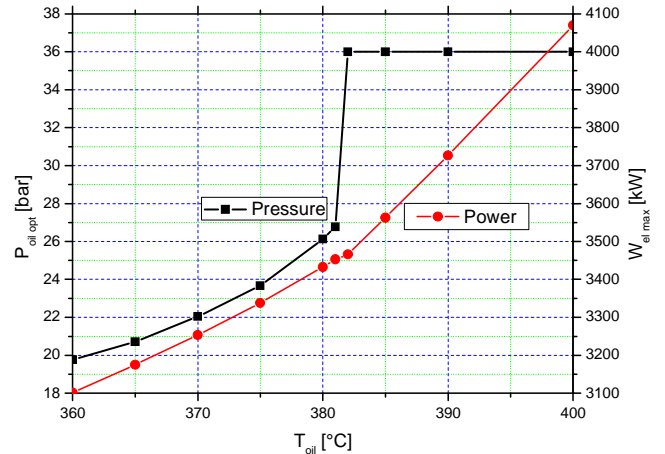


FIGURE 14: OIL TEMPERATURE VERSUS MAXIMUM OIL PRESSURE AND MAXIMUM ELECTRIC POWER.

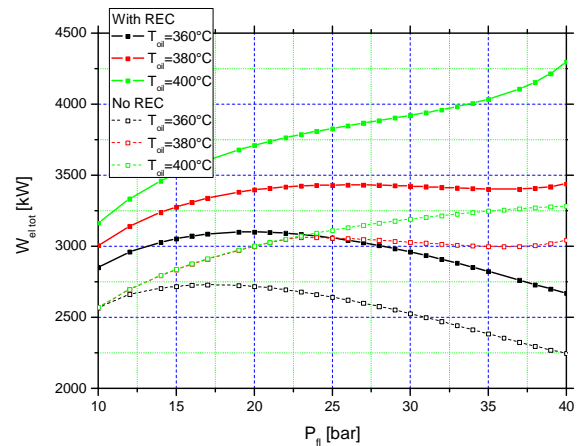


FIGURE 15: ELECTRIC OUTPUT POWER VERSUS EXPANDER INLET PRESSURE AND OIL TEMPERATURE IN DIFFERENT LAYOUT

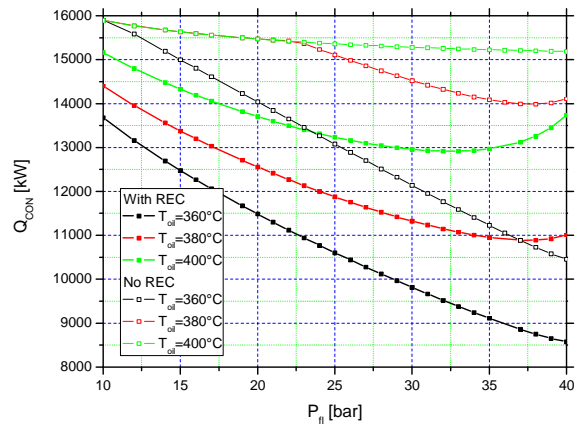


FIGURE 16: TRANSFERRED HEAT VERSUS EXPANDER INLET PRESSURE AND OIL TEMPERATURE IN DIFFERENT LAYOUT AT THE CONDENSER.

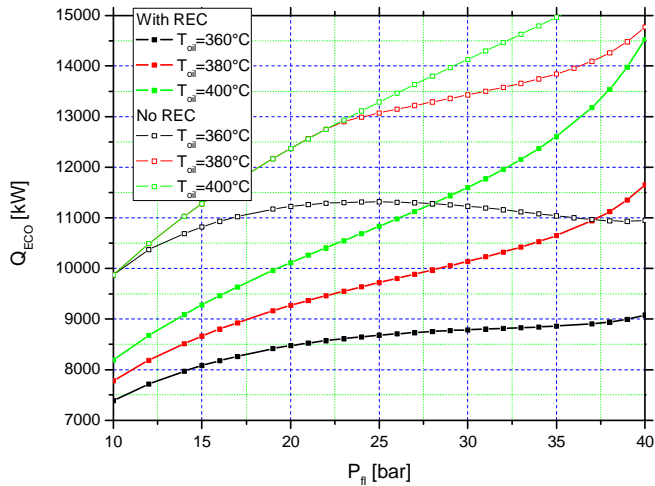


FIGURE 17: TRANSFERRED HEAT VERSUS EXPANDER INLET PRESSURE AND OIL TEMPERATURE IN DIFFERENT LAYOUT AT THE ECONOMIZER.

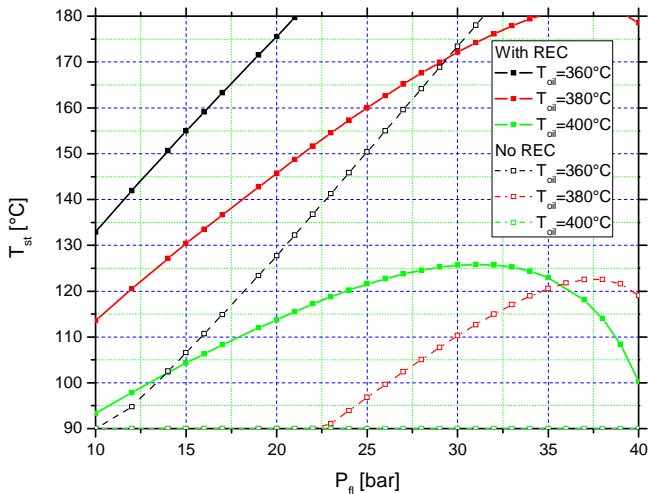


FIGURE 18: STACK TEMPERATURE VERSUS EXPANDER INLET PRESSURE AND OIL TEMPERATURE IN DIFFERENT LAYOUT AT THE ECONOMIZER.

Without the superheater the cycle has an upper pressure limit. In fact, the fluid pressure must be less than the pressure where the entropy of the saturation condition is maximum, otherwise, during the expansion, the organic fluid goes across the saturation curve and grows liquid. So the maximum working pressure is about 36.0 bar.

Figure 8 compares the heat exchanged between the configuration with and without a superheater. If a superheater is present, more heat is exchanged in the recuperator (REC) and, consequently, the stack temperature of the hot gas is higher. The same figure helps to explain the differences between the two configurations, in fact the recuperator (REC) recovers more heat in the superheated configuration, but the trend decreases, increasing the pressure.

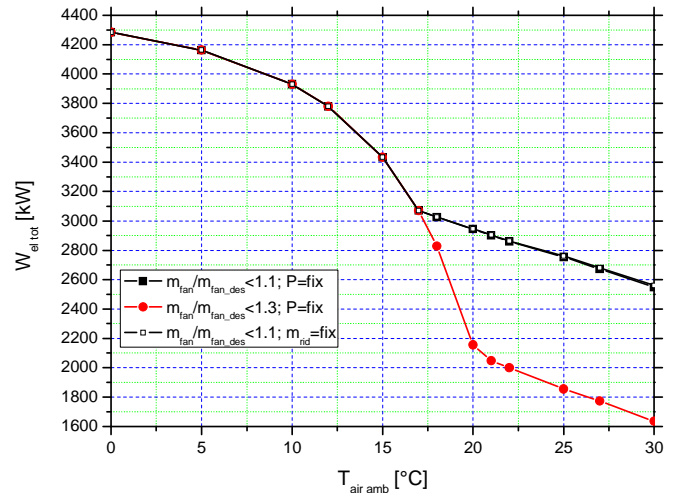


FIGURE 19: NET ELECTRIC POWER VERSUS AMBIENT TEMPERATURE

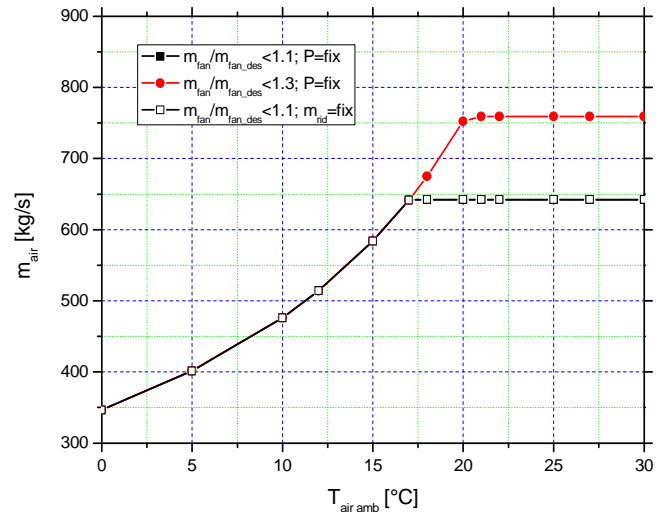


FIGURE 20: AIR MASS FLOW RATE VERSUS AMBIENT TEMPERATURE

Oil Maximum Temperature Analysis

In the previous section, an organic Rankine cycle configuration has been studied and a heat recovery unit without a superheater has been presented as the best condition. The analysis continues without superheater. A comparison between several maximum oil temperatures is carried out.

The output power increases with an increase in oil temperature (figure 9). The oil can recover more heat from the hot gas and the stack temperature decreases until the limit fixed at $T_{st_lim}=90^{\circ}\text{C}$ (figure 10). Figure 11 shows how a high oil temperature lowers the oil mass flow value; the toluene mass flow rate increases due to the higher oil temperature (figure 12).

Figure 13 compares the heat exchanged between two different values of the inlet pressure at the expander. When the

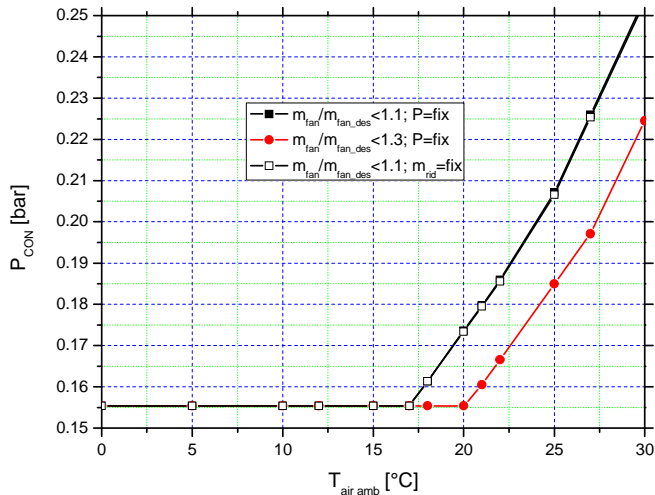


FIGURE 21: CONDENSER PRESSURE VERSUS AMBIENT TEMPERATURE

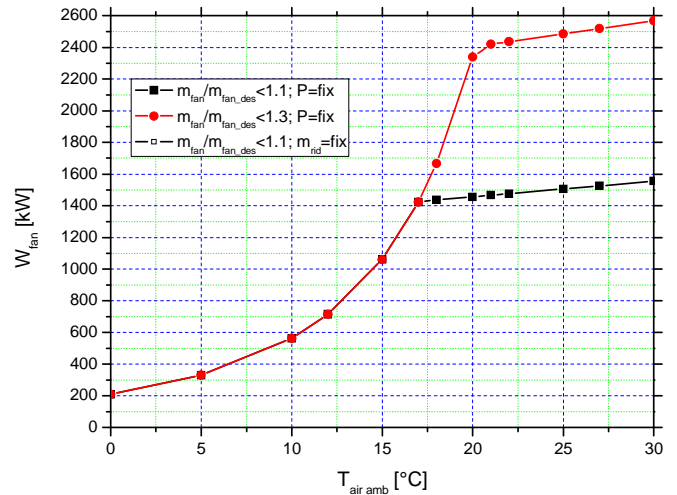


FIGURE 23: ABSORBED FAN POWER VERSUS AMBIENT TEMPERATURE

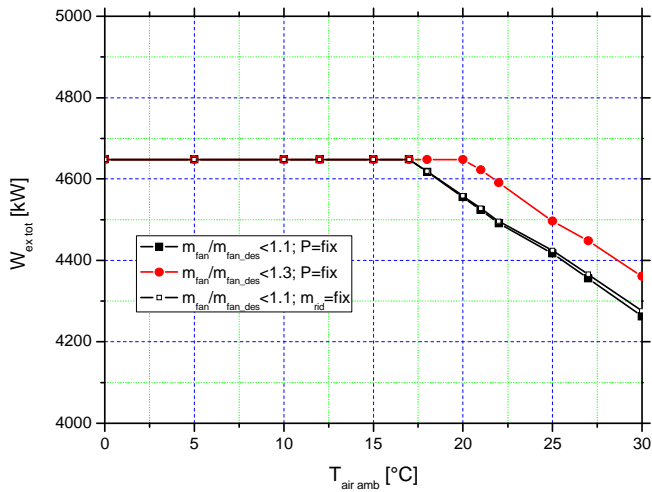


FIGURE 22: EXPANDER OUTPUT POWER VERSUS AMBIENT TEMPERATURE

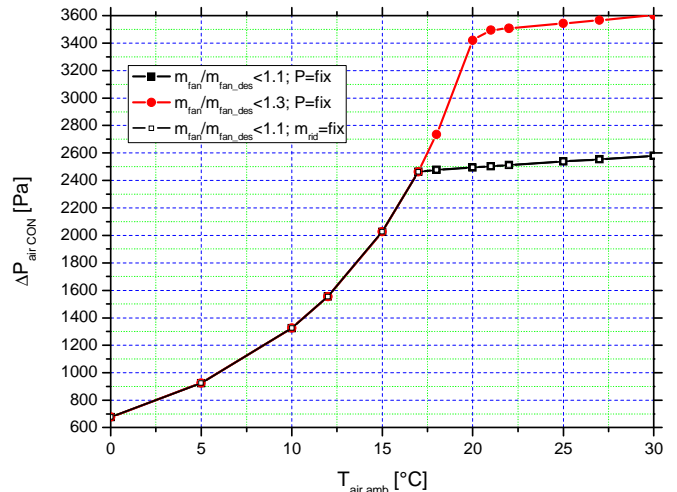


FIGURE 24: AIR PRESSURE DROP AT THE CONDENSER VERSUS AMBIENT TEMPERATURE

inlet pressure decreases, the fluid saturation temperature decreases too, but the heat exchanged in into the evaporator increases, so the heat recovery in the economizer decreases. This figure can help to explain the trend of the not superheated trend of the heat in the recuperator (REC).

Every oil temperature has a maximum value of power for the fluid pressure (figure 9), so the optimized pressure and maximum electric output power for each oil temperature can be plotted (figure 14). This figure permits to determine the best condition for each oil temperature. When the oil temperature reaches about 382°C, the optimized pressure presents a gap because the maximum of the power is near the maximum value of the fluid entropy in the T-S diagram (the pressure is limited to 36.0 bar).

Fixing the maximum oil temperature at 380°C, the optimized fluid pressure is around 26.13 bar.

Recuperator Consideration

The exhaust toluene from the expander presents a high enthalpy. The recuperator (REC) transfers this heat to the cold toluene and preheats the working fluid before the heat recovery unit. Without the recuperator (REC), the output power decreases in all cases (figure 15). In this case, the condenser receives a hotter fluid than the configuration with the recuperator and the condenser transfers a large part of the heat to the ambient air (figure 16). The economizer receives a colder working fluid and so more heat is exchanged (figure 17). The diathermic oil goes into the gas HRB colder than the other configuration and it can recover more heat, so the stack temperature decreases (figure 18). Attention must be paid to the stack temperature because, in the configuration without a

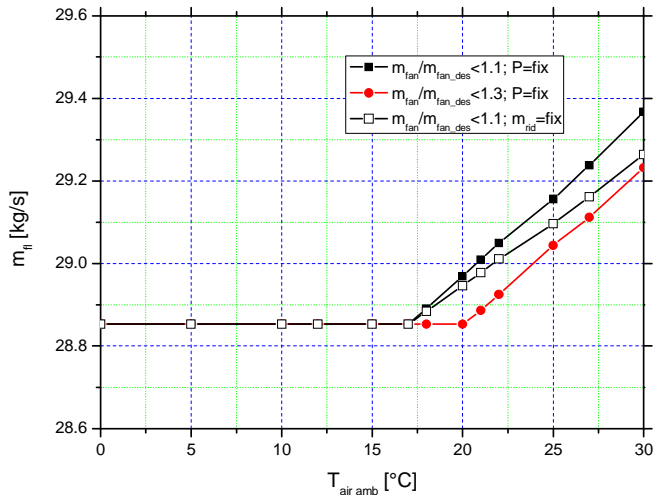


FIGURE 25: TOLUENE MASS FLOW RATE VERSUS AMBIENT TEMPERATURE

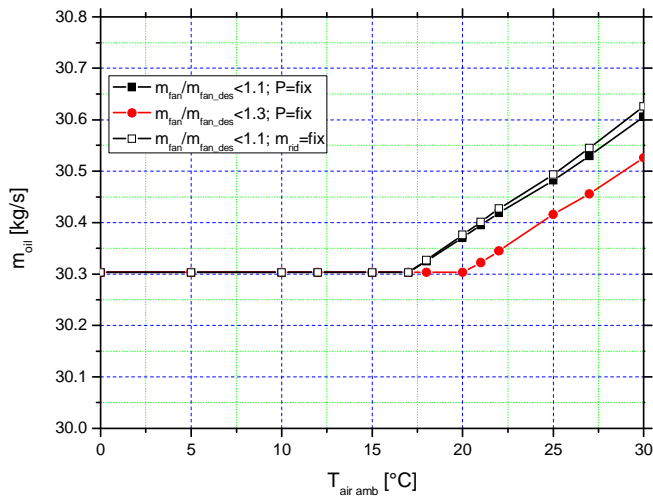


FIGURE 26: OIL MASS FLOW RATE VERSUS AMBIENT TEMPERATURE

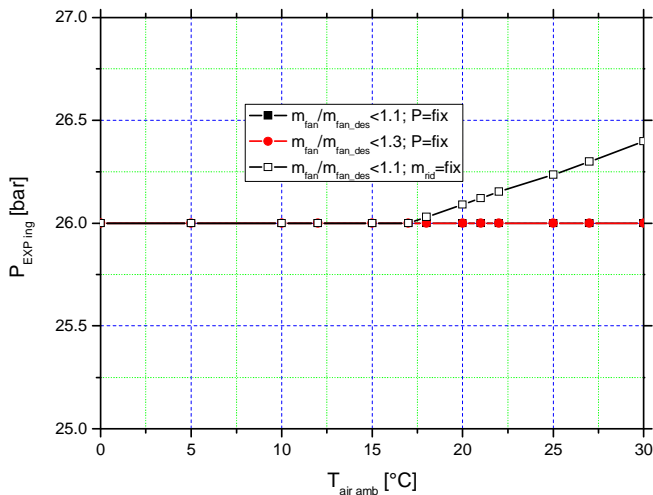


FIGURE 27: TOLUENE INLET PRESSURE AT THE EXPANDER VERSUS AMBIENT TEMPERATURE

gas temperature.

At last, more heat is recovered in the HRB, but more heat is discharged into the condenser.

OFFDESIGN CONSIDERATION

At the end of the study, an off-design analysis, varying the ambient air temperature, is presented. The aim of this part of the study is to show how the selected configuration follows ambient variation. To conduct this study, the best configuration (without superheater, with recuperator, $P_B=T_{oil}=380^\circ\text{C}$, $P_1=P_{ex_in}=26.13$ bar) selected in the previous $P_B=T_{oil}=380^\circ\text{C}$, $P_1=P_{ex_in}=26.13$ bar) selected in the previous paragraph has been chosen. The impact of the condenser behavior on the whole cycle is considered. When the ambient temperature varies, the control system of the condenser tends to impose the design pressure condenser ($P_{CON}=0.156$ bar), so when the ambient temperature increases, the air mass flow rate tends to increase, too. However, the air mass flow rate reaches the maximum value allowed by the condenser fan. To conduct this investigation, two different air mass flow ratio limits at the condenser fan are considered ($m_{fan}/m_{fan_des}\leq 1.1; 1.3$ – in the next figures, the data until 17°C circa of the ambient air temperature are overlapped for some values the data are overlapped) to verify the operability range of the condenser. The study is conducted imposing two different conditions in the expander: with a constant value of the toluene mass flow and with a constant toluene non-dimensional mass flow in the expander (EX).

Figure 19 shows the net electric power output (W_{el_tot}), which decreases with the increasing ambient temperature (T_{amb}). By varying the ambient temperature (T_{amb}) and exploiting a fixed P_{CON} , the air mass flow (figure 20) in the condenser increases and the ΔT_{air} decreases. This condition occurs until the fan operation limit is verified, so when the ambient temperature increases, the air mass flow rate is imposed at its maximum value, and the condenser pressure ($P_{CON}=P_3$) increases (figure 21). The net electric output power (W_{el_tot}) is based on two different factors: the output power from the expander (W_{ex}) and the power absorbed from the fan of the condenser (W_{fan}). The output expander power (figure 22) is quite constant until the air mass flow rate at the condenser reaches the maximum value, then it decreases because the condenser pressure (P_{CON}) increases. On the other hand, the absorbed fan power (W_{fan} - figure 23) increases drastically, especially due to two different contributions: the increase of the air mass flow (figure 20) and the increase of the pressure loss (figure 24); in fact, when the air mass flow rate increases, the pressure loss increases, too. When the air mass flow rate limit occurs, the air pressure drop becomes quite constant.

The non-dimensional mass flow depends only on the inlet conditions of the expander (EX), so it presents negligible effects with regard to the condenser thermodynamic parameters (figures 19-23). Only a minimum variation is present in the expander output power (figure 22).

The toluene mass flow is almost constant until the fan limit (figure 25). When the fan reaches its air mass flow limit, the toluene mass flow rate (m_f) increases, because the recovered heat increases in the regenerator (REC). Consequently, the oil mass flow increases, too (figure 26).

Imposing a non-dimensional mass flow rate at the expander as a constant, when the air mass flow rate reaches the maximum value, the toluene inlet expander pressure tends to increase (figure 27), because the toluene mass flow rate has increased (figure 25).

CONCLUSION

In the present paper a potential organic Rankine cycle based on toluene is investigated. In the first section, a design analysis is conducted selecting the best configuration for the selected working fluid, in terms of plant layout and thermodynamic parameters. The use of the superheater is evaluated to carry the working fluid into the superheating zone. After that, the influence of the regenerator to recover heat from the exhaust working fluid, is analyzed. Subsequently, an investigation to select the best working conditions in terms of diathermic oil temperature and expander inlet pressure is conducted.

The main conclusions of the design analysis are:

- An ORC plant analysis based on toluene, offers the best conditions in a regenerative not-superheated layout, if the expansion line does not cross the saturation curve.
- The recuperator must be in the layout. Without this component more heat is discharged in the condenser and the hot gas temperature at the stack tends to be too low.
- A higher value of the maximum oil temperature allows to recover more heat and to produce more power, but the stack temperature is very low, so its limit can be reached. It is necessary to evaluate the fuel type to choose the right value of the stack temperature (T_{st}) in order to avoid acid condensate.
- For a maximum oil temperature of 380°C, the best inlet expander pressure is about 26.13 bar.

For the off-design investigation, the behavior of the cycle is evaluated by varying the ambient temperature. Attention is mainly focused on the behavior of the condenser.

For the off-design analysis, the conclusions are:

- The ORC is very sensitive to the variation of the ambient temperature. An adequate regulation system to control the whole plant is necessary.
- The analysis is conducted with different ranges of operability ($m_{fan}/m_{fandes}=1.1$; $m_{fan}/m_{fandes}=1.3$) in the fan condenser. The condenser with a low

range of operability offers the best results for the cycle.

- The partial-load output decreases regularly until the condenser limit is reached, and then it decreases slightly.
- At the operation limit of the condenser, the condenser pressure and the toluene mass flow increase significantly, while the operability decreases.
- The power absorbed by the fan increases due the increase in air mass flow and air pressure loss. A condenser with a whole operability range reduces the output of the bottoming cycle significantly. An ORC power plant of this kind needs an efficient control system to prevent malfunction.

REFERENCES

1. C.E. Cong, S. Velautham, A.M. Darus, Sustainable power: solar thermal driven organic Rankine cycle, in: Proceedings of the International Conferences on Recent Advances in Mechanical and Materials Engineering, Paper No. 91, Kuala Lumpur, Malaysia, May 2005, pp. 424–429.
2. Hung, T.C., T.Y. Shai, S.K. Wang, A review of organic rankine cycles (ORCs) for the recovery of low grade waste heat, *Energy* 22 (7) (1997) 661-667
3. Carcasci, C., Facchini, B., Harvey, S., 1998; "Modular Approach to Analysis of Chemically Recuperated Gas Turbine Cycles", *Energy Conversion & Management*, Vol.39, n. 16-18, pp.1693-1703.
4. Carcasci, C., Facchini, B., and Harvey, S.;1998 "Design Issues and Performance of a Chemically Recuperated Aero derivative Gas Turbine", Proceedings of the Institution of Mechanical Engineers. Part A, Journal of power and energy, Vol.212, Part A, pp.315-329
5. Badr O, Ocallaghan PW, et al. Rankine-cycle systems for harnessing power from low-grade energy-sources. *Appl Energy* 1990;36(4):263–92.
6. Gu W, Weng Y, Wang Y, Zheng B. Theoretical and experimental investigation of an organic Rankine cycle for a waste heat recovery system. *Proc IMechE, Part A: J Power Energy* 2009;223:523–33.
7. Dai YP, Wang JF, et al. Parametric optimization and comparative study of organic Rankine cycle (ORC) for low grade waste heat recovery. *Energy Convers Manage* 2009;50(3):576–82.
8. J.P. Roy, M.K. Mishra, Ashok Misra Parametric optimization and performance analysis of a waste heat recovery system using Organic Rankine Cycle *Energy* 35 (2010) 5049e5062
9. Yiping Dai, Jiangfeng Wang *, Lin Gao Parametric optimization and comparative study of organic

- Rankine cycle (ORC) for low grade waste heat recovery *Energy Conversion and Management* 50 (2009) 576–582
10. Gnutek Z, Bryszewska-Mazurek A. The thermodynamic analysis of multicycle ORC engine. *Energy* 2001;26(12):1075–82.
 11. Chen Y, Lundqvist P, et al. A comparative study of the carbon dioxide transcritical power cycle compared with an organic rankine cycle with R123 as working fluid in waste heat recovery. *Appl Therm Eng* 2006;26(17–18):2142–7.
 12. P. Gang, Li Jing, Ji Jie "Analysis of low temperature solar thermal electric generation using regenerative Organic Rankine Cycle." *Applied Thermal Engineering* 30 (2010) 998–1004
 13. S. Quoilin a, M. Orosz b, H. Hemond b, V. Lemort a Performance and design optimization of a low-cost solar organic Rankine cycle for remote power generation *Solar Energy* (2011)
 14. G. Kosmadakis, D. Manolakos, G. Papadakis Simulation and economic analysis of a CPV/thermal system coupled with an organic Rankine cycle for increased power generation *Solar Energy* 85 (2011) 308–324
 15. Florian Heberle*, Dieter Brüggemann Exergy based fluid selection for a geothermal Organic Rankine Cycle for combined heat and power generation. *Applied Thermal Engineering* 30 (2010) 1326 - 1332
 16. M. Astolfi, L. Xodo, M. C. Romano, E. Macchi Technical and economical analysis of a solar-geothermal hybrid plant based on an Organic Rankine Cycle. *Geothermics* 40 (2011) 58–68
 17. D. Sanchez, J.M. Muñoz de Escalona, B. Monje, R. Chacartegui, T. Sanchez Preliminary analysis of compound systems based on high temperature fuel cell, gas turbine and Organic Rankine Cycle. *Journal of Power Sources* 196 (2011) 4355–4363
 18. R. Chacartegui, D. Sánchez, J.M. Muñoz, T. Sánchez Alternative ORC bottoming cycles FOR combined cycle power plants *Applied Energy* 86 (2009) 2162–2170
 19. J.M. Muñoz de Escalona, D. Sánchez, R. Chacartegui, T. Sánchez "Part-load analysis of gas turbine & ORC combined cycles" *Applied Thermal Engineering* 36 (2012) 63e72
 20. N. A. Lai, M. Wendland, J. Fischer Working fluids for high-temperature organic Rankine cycles *Energy* 36 (2011) 199e211
 21. B. Saleh, G. Koglbauer, M. Wendland, J. Fischer Working fluids for low-temperature organic Rankine cycles *Energy* 32 (2007) 1210–1221
 22. Vankeirsbilck I.1, Vanslambrouck B.*1, Gusev S.1, De Paepe M. Organic Rankine Cycle As Efficient Alternative To Steam Cycle For Small Scale Power Generation 8th International Conference on Heat Transfer, Fluid Mechanics and Thermodynamics
 23. U. Drescher, D. Brüggemann Fluid selection for the Organic Rankine Cycle (ORC) in biomass power and heat plants *Applied Thermal Engineering* 27 (2007) 223–228
 24. N. B. Desai, S. Bandyopadhyay Process integration of organic Rankine cycle *Energy* 34 (2009) 1674–1686
 25. Quoilin, S., Lemort, V., Lebrun, J., 2010. Experimental study and modeling of an organic rankine cycle using scroll expander. *Appl. Energy* 87, 1260–1268.
 26. James AM, Jon RJ, Jiming Cao, Douglas KP, Richard NC. Experimental testing of gerotor and scroll expanders used in, and energetic and exergetic modeling of, an Organic Rankine Cycle. *J Energy Res Technol* 2009;131:012201–8.
 27. Manolakosa D, Papadakisa G, Kyritsisa S, Bouzianasb K. Experimental evaluation of an autonomous low-temperature solar Rankine cycle system for reverse osmosis desalination. *Desalination* 2007;203:366–74.
 28. Aoun B, Clodic D. Theoretical and experimental study of an oil-free scroll type vapor expander. In: Proc. the 19th Int. compressor engineering conference at Purdue, paper 1188; 2008.
 29. Peterson RB, Wang H, Herron T. "Performance of a small-scale regenerative Rankine power cycle employing a scroll expander." *Proc. IMechE. Part A: J Power Energy* 2008;vol. 222:271–82.
 30. Mathias JA, Johnston J, Cao J, Priedeman DK, Christensen RN. "Experimental testing of gerotor and scroll expanders used in, and energetic and exergetic modeling of, an organic Rankine cycle". *Journal of Energy Resources Technology* 2009;131(3):012201–12209.
 31. P. Del Turco, A. Asti, A.S. Del Greco, A. Bacci, G. Landi, G. Seghi 2011; "The ORegen™ waste heat recovery cycle: Reducing the CO2 footprint by means of overall cycle efficiency improvement" *ASME Turbo Expo* 2011.
 32. Dow Chemical Company Product Line Guide May 2007 www.dowtherm.com
 33. Nuovo Pignone GE Oil & Gas GE10 – 1 Gas Turbine 2005 Brochure www.ge.com/oil&gas
 34. F. Incropera D. P. DeWitt *Fundamentals of Heat and Mass Transfer* 1981 John Wiley & Sons, Inc.
 35. S. H. Kang Design and experimental study of ORC (organic Rankine cycle) and radial turbine using R245fa working fluid *Energy* April 2012
 36. H. Lukowicz, A Kochaniewicz Analysis of the use of waste heat obtained from coal-fired units in Organic Rankine Cycles and for brown coal drying *Energy* 9 April 2012